Vibrational studies of $A(B'_{2/3}B''_{1/3})O_3$ perovskites (A = Ba, Sr; B' = Y, Sm, Dy, Gd, In; B'' = Mo, W)

2004 J. Phys.: Condens. Matter 16 2297

(http://iopscience.iop.org/0953-8984/16/13/010)

INSTITUTE OF PHYSICS PUBLISHING JOURNAL OF PHYSICS: CONDENSED MATTER

J. Phys.: Condens. Matter **16** (2004) 2297–2310 PII: S0953-8984(04)71888-3

Vibrational studies of $A(B'_{2/3}B''_{1/3})O_3$ perovskites (A = Ba, Sr; B′ = Y, Sm, Dy, Gd, In; B″ = Mo, W)

M Mączka[1], J Hanuza[1,2], A F Fuentes[3] and Y Morioka[4]

[1] Institute of Low Temperature and Structure Research, Polish Academy of Sciences, PO Box 1410, 50-950 Wrocław 2, Poland
[2] Department of Bioorganic Chemistry, Faculty of Industry and Economics, Wrocław University of Economics, 118/120 Komandorska Street, 53-345 Wrocław, Poland
[3] CINVESTAV-IPN Unidad Saltillo, Carretera Saltillo-Monterrey Km. 13, Apartado Postal 663, 25000-Saltillo, Coahuila, Mexico
[4] Department of Chemistry, Faculty of Science, Saitama University, Shimo-Okubo 255, Urawa, 338-8570, Japan

E-mail: maczka@int.pan.wroc.pl

Received 14 November 2003, in final form 30 January 2004
Published 19 March 2004
Online at stacks.iop.org/JPhysCM/16/2297 (DOI: 10.1088/0953-8984/16/13/010)

Abstract

The Raman- and IR-active phonons were studied in ordered $Ba(Y_{2/3}Mo_{1/3})O_3$, $Ba(Y_{2/3}W_{1/3})O_3$, $Ba(Gd_{2/3}W_{1/3})O_3$, $Ba(Sm_{2/3}W_{1/3})O_3$, $Ba(Dy_{2/3}W_{1/3})O_3$, $Ba(Dy_{2/3}Mo_{1/3})O_3$ and $Ba(In_{2/3}W_{1/3})O_3$ as well as disordered $Ba(In_{2/3}Mo_{1/3})O_3$ and $Sr(In_{2/3}W_{1/3})O_3$. The assignment of the observed modes was given on the basis of lattice dynamical calculations. The studies performed revealed the presence of forbidden by the selection rules Raman bands for the $Ba(In_{2/3}Mo_{1/3})O_3$ sample. This result suggests that the $Ba(In_{2/3}Mo_{1/3})O_3$ contains 1:1 ordered domains of $Fm\bar{3}m$ symmetry embedded in the disordered $Pm\bar{3}m$ matrix and that $Ba(In_{2/3}Mo_{1/3})O_3$ and $Ba(In_{2/3}W_{1/3})O_3$ may be obtained in both ordered and disordered structures, depending on the thermal treatment. This behaviour resembles that of well known $Pb(In_{1/2}Nb_{1/2})O_3$, $Pb(Sc_{1/2}Nb_{1/2})O_3$ and $Pb(Sc_{1/2}Ta_{1/2})O_3$ relaxors.

1. Introduction

Perovskites have been extensively studied due to their interesting physicochemical properties. For example, $Pb(B'_{1-x}B''_x)O_3$ perovskites, where B′ = Mg, Zn, Sc, In, Fe and B″ = Nb, Ta, W, are well known relaxor ferroelectrics [1], whereas $Ln_{1-x}A_xMnO_3$ type perovskites (Ln = rare earth, A = alkali earth) are famous due to their colossal magnetoresistance [2]. The structure of the ideal simple ABO_3 perovskite is cubic, $Pm\bar{3}m$. In the complex perovskite structure two limiting cases can be distinguished. First, the distribution of cations among octahedral sites is random and the structure can still be described by the $Pm\bar{3}m$ space group. Second, the cations are ordered. As a result the lattice parameter doubles, in comparison with the simple

perovskite, and the structure is described by the $Fm\bar{3}m$ space group. In addition to these two cases, the symmetry lowering of the cubic structure may occur. Moreover, crystals may exhibit different degrees of short-range order forming ordered nanodomains spread inside a disordered matrix [1].

Data analysis of more than 300 perovskites showed that the random distribution of cations among octahedral sites can be realized only when the ionic radii difference is less than 0.2 Å and the charge difference is 2 [3]. However, our recent structural studies revealed, surprisingly, that, in spite of the +3 charge difference and a 0.2 Å difference in ionic radii, $Ba(In_{2/3}Mo_{1/3})O_3$ and $Sr(In_{2/3}W_{1/3})O_3$ crystallize in a disordered structure whereas two forms, one ordered and another disordered, coexist at room temperature for $Ba(In_{2/3}W_{1/3})O_3$ [4]. This behaviour indicates that the chemical differences between In and W, and possibly also between In and Mo, are close to the critical limit for B-site disorder/order occupancy and that it could be possible to modify the degree of order by appropriate thermal treatment. In this respect the indium-containing perovskites discussed here resemble $Pb(In_{1/2}Nb_{1/2})O_3$, $Pb(Sc_{1/2}Nb_{1/2})O_3$ and $Pb(Sc_{1/2}Ta_{1/2})O_3$ [1]. Since it is well known that properties of $A(B'_{1-x}B''_x)O_3$ complex perovskites featuring two different ions sharing the B sites may be strongly affected by order/disorder phenomena involving the B ions, it is important to study the degree of order in perovskites. In the present paper IR and Raman spectroscopies, which are powerful techniques for probing short-range order and the local environment [1, 5], have been used for characterization of the above-mentioned disordered In(III) perovskites. The results obtained are compared with vibrational properties of ordered Dy, Gd, Y and Sm perovskites. The experimentally determined Raman and IR wavenumbers have been also compared to results of lattice dynamical calculations. This allowed us to assign the observed bands to respective motions of atoms in the unit cell. We would like to emphasize that the present studies concern the $A(B'_{2/3}B''_{1/3})O_3$ group of perovskites, for which very scarce data are available. In this group the ratio of the lower valence state element B′ (trivalent in the present case) to the higher valence state element B″ (hexavalent in the present case) is 2:1 whereas the most extensively studied perovskites are characterized by the B′:B″ ratio of 1:1 or 1:2. To the authors' knowledge the only well known compound belonging to the $A(B'_{2/3}B''_{1/3})O_3$ group is $Pb(Fe_{2/3}W_{1/3})O_3$, famous due to its relaxor ferroelectric properties [6, 7]. It is also worth noting that no IR and Raman studies have been reported so far for any member of this group of complex perovskites. The present studies provide, therefore, valuable information on order/disorder phenomena and the lattice dynamics of these materials.

2. Experimental details

The titular compounds were obtained by the polymeric precursors method, first described by Pechini to obtain alkaline-earth titanates and niobates [8]. The starting chemicals were hydrated metal nitrates, barium carbonate, strontium nitrate, ammonium paratungstate and ammonium dimolybdate. Chemicals were weighed in the appropriate stoichiometric ratios and dissolved in a citric acid solution with gentle heating and continuous stirring until a clear solution was obtained. Ethylene glycol, added to the solutions to promote polymerization of the metal citrates by a polyesterification reaction, and prolonged heating at 90–100 °C to evaporate water molecules produced in all cases white gels. On drying at 150 °C for 5 h, these gels yielded highly porous solid resins which were ground and thermally treated in high alumina crucibles for 16 h at 1200 °C (heating rate 10 °C min^{-1}). X-ray powder diffraction patterns taken after this thermal treatment were typical of a perovskite type of structure although small amounts of barium tungstates or molybdates of different stoichiometry were also present in some cases as impurities. Thermal treatments continued until undesired phases were removed or no changes

were observed in the sample XRD powder patterns collected after two consecutive thermal treatments, assuming then that the system was at equilibrium. A detailed description of the methodology followed for the synthesis of the titular compounds can be found elsewhere [4, 9].

Back-scattering Raman spectra, except for $Ba(In_{2/3}W_{1/3})O_3$ and $Ba(In_{2/3}Mo_{1/3})O_3$, were recorded with a Bruker FT-Raman RFS 100/S spectrometer. Excitation was performed with a YAG:Nd^{3+} laser. Blackman–Harris four-term apodization was applied and the number of collected scans was 64. The spectra of the $Ba(In_{2/3}W_{1/3})O_3$ and $Ba(In_{2/3}Mo_{1/3})O_3$ could not be recorded with YAG:Nd^{3+} laser excitation due to a strong fluorescence background. The Raman spectra of these compounds were, therefore, measured with a Jobin Yvon T64000 spectrometer, equipped with N_2-cooled charge coupled device (CCD) detection system. The 488 nm line of a mixed ArKr ion laser (Spectra Physics) was used as excitation.

Polycrystalline infrared spectra were measured with a Biorad 575C FT-IR spectrometer with Nujol suspension. 128 scans were collected in the mid-IR region and a triangular apodization was applied. In the far-IR region medium Norton–Beer apodization was used and the number of scans was 256. The IR and Raman spectra were recorded with a spectral resolution of 2 cm^{-1}.

3. Results and discussion

To make the discussion of the results easier, an acronym made up of the first letter of the chemical symbol of the four elements involved in every composition will be assigned to each phase. That is, $Ba(In_{2/3}Mo_{1/3})O_3$ would be represented by BIMO, $Ba(In_{2/3}W_{1/3})O_3$ by BIWO, $Ba(Y_{2/3}Mo_{1/3})O_3$ by BYMO, $Ba(Y_{2/3}W_{1/3})O_3$ by BYWO, $Ba(Gd_{2/3}W_{1/3})O_3$ by BGWO, $Ba(Sm_{2/3}W_{1/3})O_3$ by BSWO, $Ba(Dy_{2/3}W_{1/3})O_3$ by BDWO, $Ba(Dy_{2/3}Mo_{1/3})O_3$ by BDMO and $Sr(In_{2/3}W_{1/3})O_3$ by SIWO.

An HREM and XRD characterization of the titular compounds revealed that all of them were cubic except for the strontium-containing compound, SIWO (see table 1) [4, 9]. Interestingly enough, our previous HREM and XRD studies showed that BIMO and SIWO present a random distribution of In and W or Mo over the octahedral sites while BIWO was found to be a mixture of two forms, one ordered (SG $Fm\bar{3}m$) accounting for around 70% of the sample weight and another one, disordered (SG $Pm\bar{3}m$), 21% weight [4]. The remaining compounds, as expected from large differences in charge and size between the two ions sharing the octahedral positions, were found to present an ordered distribution of B′(III) and B″(VI) [9].

3.1. Description of the model used in the lattice dynamical calculations

The calculations of wavenumbers and displacement vectors were performed on the basis of a partially ionic model described previously [10]. The atomic positions used in the calculations were taken from [4, 9]. The following potential was used in these calculations:

$$U_{ij}(r_{ij}) = z_i z_j e^2/r_{ij} + (b_i + b_j)\exp[(a_i + a_j - r_{ij})/(b_i + b_j)] - c_i c_j/r_{ij}^6 + D_{ji}(\exp[-2\beta_{ij}(r_{ij} - r_{ij}^*)] - 2\exp[-\beta_{ij}(r_{ij} - r_{ij}^*)]).$$

This potential consist of a Coulomb interaction (first term), Born–Mayer type repulsive interaction (second term), van der Waals attractive interaction (third term) and the Morse potential contribution (last term). z_i and z_j are the effective charges of the ions i and j, respectively, separated by a distance r_{ij}. The parameters a_i, a_j and b_i, b_j correspond to the ionic radius and ionic stiffness, respectively. For the 4b site, occupied by both B′ = Y, Sm, Gd, Dy, Y, In and B″ = Mo, W in a ratio of 1:2, the mass of the artificial atom B with $m_B = 1/3m_{B'} + 2/3m_{B''}$ was used. The parameters used in the present calculations are listed

Table 1. Structural characteristics of $A(B'_{2/3}B''_{1/3})O_3$ (A = Ba or Sr; B′ = In, Y, Dy, Gd and Sm; B″ = W or Mo) complex perovskites.

Phase	Symmetry	Cell parameters (Å)	Cell volume, V (Å^3)
$Ba(In_{2/3}Mo_{1/3})O_3$	Cubic (SG $Pm\bar{3}m$)	$a = 4.166\,06(3)$	72.306(2)
$Ba(In_{2/3}W_{1/3})O_3$	Cubic (SG $Pm\bar{3}m$) (21% weight)	$a = 4.157\,3(1)$	71.85(1)
	Cubic (SG $Fm\bar{3}m$) (70% weight)	$a = 8.315\,0(2)$	574.90(2)
$Sr(In_{2/3}W_{1/3})O_3$	Orthorhombic (SG $Pnma$)	$a = 5.767\,3(2)$ $b = 8.141\,3(3)$ $c = 5.754\,1(2)$	270.18(2)
$Ba(Y_{2/3}Mo_{1/3})O_3$	Cubic (SG $Fm\bar{3}m$)	$a = 8.501\,7(2)$	614.50(3)
$Ba(Y_{2/3}W_{1/3})O_3$	Cubic (SG $Fm\bar{3}m$)	$a = 8.509\,3(3)$	616.14(4)
$Ba(Dy_{2/3}Mo_{1/3})O_3$	Cubic (SG $Fm\bar{3}m$)	$a = 8.527\,8(3)$	620.17(4)
$Ba(Dy_{2/3}W_{1/3})O_3$	Cubic (SG $Fm\bar{3}m$)	$a = 8.527\,6(3)$	620.14(3)
$Ba(Gd_{2/3}W_{1/3})O_3$	Cubic (SG $Fm\bar{3}m$)	$a = 8.581\,7(3)$	632.00(3)
$Ba(Sm_{2/3}W_{1/3})O_3$	Cubic (SG $Fm\bar{3}m$)	$a = 8.622\,6(3)$	641.09(4)

in table 2. We consider covalency for the B–O bonds only. The values of the parameters for O are taken from [10]. The values of the parameters b for the rare earth and indium atoms were assumed to be the same as that found for La and were taken from [10]. Since the parameters a reflect the radii, they were obtained for the B′ = Y, Sm, Gd, Dy, In atoms using the value for the La atom reported in [10], i.e. $a_{B'} = a_{La}r_{B'}/r_{La}$, where r denotes the ionic radius. Initial parameters for the Ba^{2+} cations were assumed to be the same as that found in the study of $BaTiO_3$ [11]. Finally, the initial parameters a, b, D_{ij}, β_{ij} and r^*_{ij} used for the artificial B atoms were taken to be the same as those found for the Ti^{4+} ions [10]. These initial parameters for the B and Ba atoms were changed during the calculations to obtain the best agreement between the observed and calculated wavenumbers.

3.2. Rare earth and yttrium perovskites

Structural studies showed that all the studied rare earth and yttrium compounds crystallize in the ordered $Fm\bar{3}m$ cubic perovskite structure [9]. In this structure crystallographic positions 4a are occupied by the B′ atoms, where B′ = Y, Gd, Sm, Dy, whereas 4b sites are occupied by both B′ and Mo or W atoms (the B′:Mo(W) ratio is 1:2). The Ba and oxygen atoms are located in the 8c and 24e sites, respectively. Since the primitive cell contains two $A(B'_{2/3}B''_{1/3})O_3$ formula units, there are 30 vibrational degrees of freedom distributed among $A_{1g} + E_g + F_{1g} + 2F_{2g} + 5F_{1u} + F_{2u}$ irreducible representations. Among these modes $F_{1g} + F_{2u}$ are both IR- and Raman-inactive and one of the F_{1u} modes corresponds to the acoustic phonon. Therefore, one should expect to observe four bands in IR ($4F_{1u}$) and four in Raman ($A_{1g} + E_g + 2F_{2g}$) spectra.

The former studies of a number of ordered perovskites $A(B'_{1/2}B''_{1/2})O_3$, where A = Ba, Sr, Pb; B′ = Mg, Ni, Co, Zn, Cd, Ca, Sc, Y, Al, lanthanide; B″ = Mo, W, Ta, Nb have shown the presence of the A_{1g} mode at 770–860 cm^{-1} [12–15]. It has been also noticed that the energy of this mode is higher for the tungstates (800–847 cm^{-1}) than for the molybdates (779–808 cm^{-1}) [12]. It has been shown previously that Mo–O stretchings are generally located at lower frequencies than W–O stretchings in isostructural compounds, irrespective of the crystal structure [16]. The E_g mode was not observed for the tungstates, possibly due to its very low intensity. However, the study of $Ba(Cd_{1/2}Mo_{1/2})O_3$, $Sr(Al_{1/2}Ta_{1/2})O_3$, $Sr(Al_{1/2}Nb_{1/2})O_3$,

Table 2. Potential parameters used in the calculations. For BIWO the first value is given for the ordered and the second for the disordered structure.

Ion	z (e)	a (Å)	b (Å)	C (kcal$^{1/2}$ Å^3 mol$^{-1/2}$)
O	−1.0	1.926	0.16	20
Y	1.4	1.201	0.09	0
Dy	1.4	1.213	0.09	0
Sm	1.4	1.272	0.09	0
Gd	1.4	1.236	0.09	0
In	1.4	0.962	0.09	0
Ba	1.4	1.630	0.08	0
Y/W	1.8	1.164	0.09	0
Y/Mo	1.8	1.124	0.09	0
Dy/W	1.8	1.174	0.09	0
Dy/Mo	1.8	1.134	0.09	0
Gd/W	1.8	1.198	0.09	0
Sm/W	1.8	1.232	0.09	0
In/W	1.8 or 1.6	0.904	0.09	0
In/Mo	1.6	0.894	0.09	0
Ion pair	**D_{ji} (kcal mol^{-1})**	**β_{ij} (Å)**	**r^*_{ij} (Å)**	
B′/W–O	28.0	2.3	2.1	
Y/Mo–O	26.0	2.3	2.1	
Dy/Mo–O	26.0	2.1	1.9	
In/W–O	26.0	2.3 or 2.25	2.1 or 2.05	
In/Mo–O	26.0	2.25	2.05	

$Sr(Ln_{1/2}Nb_{1/2})O_3$ and $Sr(Ln_{1/2}Ta_{1/2})O_3$ compounds (Ln denotes a lanthanide ion) showed that this mode is observed in the 500–580 cm^{-1} range [12, 13, 15]. The two F_{2g} modes were located at 401–446 and 104–140 cm^{-1} for the tungsten- and molybdenum-containing perovskites [12]. Finally, the four predicted IR bands were observed for the tungstates and molybdates at 590–660, 350–400, 200–350 and 100–170 cm^{-1} [12].

IR and Raman spectra are presented in figures 1 and 2. The bands in the Raman spectra denoted by asterisks have been assigned to spurious fluorescence because they are not observed in the anti-Stokes part of the spectrum (not shown in figure 1). The recorded spectra also show the presence of weak bands (denoted by arrows) attributed to a $BaMoO_4$ impurity, observed also by the XRD method. No bands, which could be attributed to a barium tungstate impurity, were identified in the spectra.

The measured spectra show that the vibrational behaviour of $A(B'_{2/3}B''_{1/3})O_3$ rare earth perovskites is very similar to the behaviour of previously studied $A(B'_{1/2}B''_{1/2})O_3$ perovskites. First, there is no band at 500–600 cm^{-1} which could be assigned to the E_g mode. Second, the most intense band in the Raman spectra is observed around 800 cm^{-1}. Third, the highest wavenumber Raman modes are observed at higher energy for the tungstates than for the molybdates. Fourth, four IR bands are observed around 560–590, 290–320, 170–220 and 110–120 cm^{-1} (see figure 2). The similarity between vibrational properties of the previously studied ordered $A(B'_{1/2}B''_{1/2})O_3$ perovskites and the presently studied $A(B'_{2/3}B''_{1/3})O_3$ compounds allows us to assign the observed bands in the same way as proposed previously [5, 12–15, 17–19]. We can assign, therefore, the highest wavenumber band at 779–824 cm^{-1} to the A_{1g} mode, which corresponds to the totally symmetric stretch of the $WO_6(MoO_6)$ octahedron (ν_1 of a free octahedron). The calculations confirm this assignment (see figure 3) and predict that the E_g mode, not observed for the samples studied, should appear in the 550–600 cm^{-1}

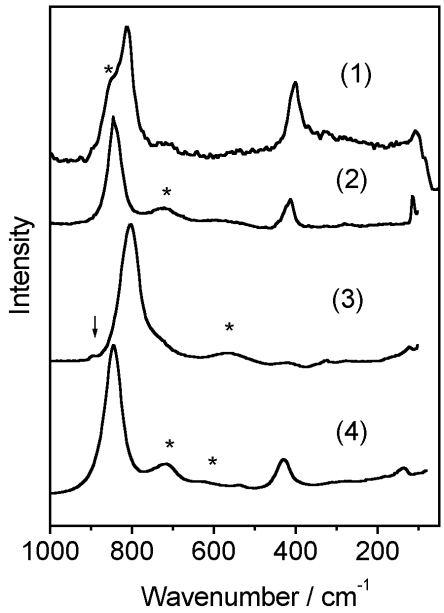

Figure 1. (1) Representative Raman spectrum of the lanthanide-containing ordered $Fm\bar{3}m$ perovskite ($Ba(Sm_{2/3}W_{1/3})O_3$) and Raman spectra of the indium-containing samples: (2) $Ba(In_{2/3}W_{1/3})O_3$, (3) $Ba(In_{2/3}Mo_{1/3})O_3$ and (4) $Sr(In_{2/3}W_{1/3})O_3$. The bands arising from some spurious fluorescence and a $BaMoO_4$ impurity are denoted by asterisks and the arrow, respectively.

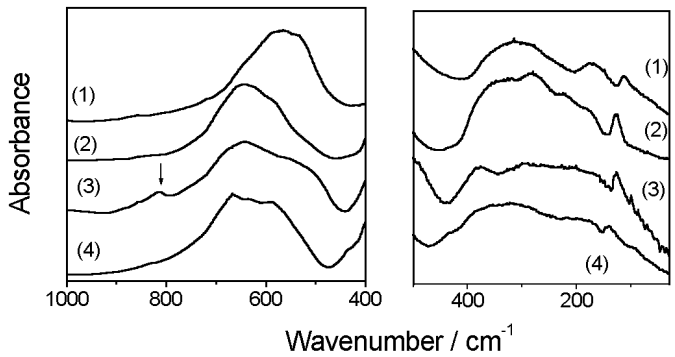

Figure 2. (1) Representative IR spectrum of the ordered $Fm\bar{3}m$ perovskite ($Ba(Gd_{2/3}W_{1/3})O_3$) and the spectra of the indium-containing samples: (2) $Ba(In_{2/3}W_{1/3})O_3$, (3) $Ba(In_{2/3}Mo_{1/3})O_3$ and (4) $Sr(In_{2/3}W_{1/3})O_3$. The band attributed to the $BaMoO_4$ impurity is denoted by the arrow.

range (see table 3). This result supports the assignment of the 510–580 cm^{-1} modes, observed for $Ba(Cd_{1/2}Mo_{1/2})O_3$, $Sr(Al_{1/2}Nb_{1/2})O_3$ and $Sr(Al_{1/2}Ta_{1/2})O_3$ [12, 13], to the E_g mode. As far as two F_{2g} modes are concerned, the factor group analysis shows that, during these vibrations hexa- and trivalent cations are necessarily at rest. These modes should be assigned, therefore, to the bending vibration of the $WO_6(MoO_6)$ group coupled with translation of the Ba^{2+} cations. Since, however, the former studies of $A(B'_{1/2}B''_{1/2})O_3$ perovskites showed much stronger wavenumber dependence on the mass of the divalent cation for the lower wavenumber mode than for the higher wavenumber mode [12–14], we may conclude that the

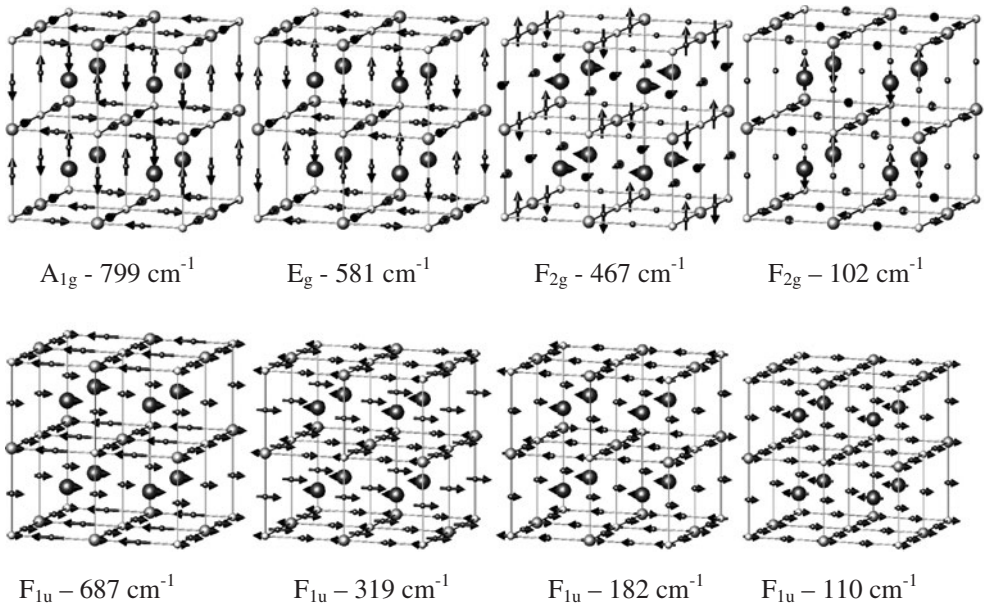

Figure 3. Calculated frequencies and displacement vectors for the representative perovskite crystallizing in the $Fm\bar{3}m$ structure ($Ba(Gd_{2/3}W_{1/3})O_3$).

bands around 100 cm^{-1} correspond predominantly to the translational motions of the Ba^{2+} cations and the bands around 400 cm^{-1} to the bending mode of the $WO_6(MoO_6)$ group (ν_5 of a free octahedron). Lattice dynamical calculations confirm this assignment since a very significant displacement of Ba^{2+} ions is predicted for the ∼100 cm^{-1} mode (see figure 3). The calculated displacement vectors (see figure 3) show also that the two higher wavenumber IR bands can be assigned to the stretching and bending modes of the $WO_6(MoO_6)$ group (ν_3 and ν_4 of a free octahedron). Regarding the remaining IR bands, our study suggests that the bands at 170–220 cm^{-1} correspond predominantly to the translations of trivalent atoms since a very clear shift from about 175 to 213–216 cm^{-1} is observed when heavy Sm, Gd or Dy atoms are replaced by much lighter Y atoms (see table 3). The calculations are consistent with this conclusion but show that this mode also involves large motions of W or Mo atoms. Finally, the calculated displacement vectors show unambiguously that the lowest wavenumber IR band corresponds predominantly to translational motions of Ba^{2+} cations (see figure 3). It is worth noting that the strong IR bands around 570 and 300 cm^{-1} show the presence of additional shoulders. These shoulders are much more pronounced for the molybdates than for the tungstates. The appearance of these shoulders due to impurities seems to be rather unlikely since the XRD studies showed that the main impurities are barium tungstates and molybdates. These impurities should have, however, the most intense bands in the 800–950 cm^{-1} region and are clearly observed in our spectra as weak bands (see figures 1 and 2). Another possible explanation of the observed shoulders is a local symmetry breakdown.

This effect should lead to activation in the IR spectra of some Raman-active modes. The observed shoulders do not correspond, however, to any Raman-active modes. The appearance of shoulders could also be attributed to a deformation of the crystal lattice. The former studies of ordered $Pb(Sc_{1/2}Ta_{1/2})O_3$ showed that a decrease in symmetry from cubic to rhombohedral gives rise to new bands on the high frequency side of the stretching and bending bands [17],

Table 3. Raman and IR wavenumbers (in cm^{-1}) for all the studied perovskites. The values in parentheses for BIWO concern the disordered structure. The L and T denotes longitudinal and transverse, respectively. vs, s, sh, m, vw and w denote very strong, strong, shoulder, medium, very weak and weak, respectively.

BSWO		BGWO		BDWO		BYWO		BDMO		BYMO		BIWO		BIMO		SIWO		
obs.	calc.	obs.	calc.	obs.	calc.	obs.	calc.	obs.	calc.	obs.	calc.	obs.	calc.	obs.	calc.	obs.	Activity	Assignment
811s	820	814s	799	822s	810	824s	814	779s	805	784s	793	842s	848	804s		844vs	Raman	Stretching (ν_1)
—	634	—	581	—	578	—	574	—	558	—	572	—	603	—	—	—	Raman	Stretching (ν_2)
								642sh		652sh								
		625sh		635sh		631sh		582sh		591sh								
	741L		702L		706L		717L		701L		705L		750L(723L)		721L	666s		Stretching (ν_3)
565s	722T	565s	687T	568s	693T	564s	702T	536s	687T	557s	686T	644s	736T(711T)	643s	708T	629s	IR	
												581sh		543sh		588s		
																438sh	Raman	Bending (ν_5)
400m	441	405s	467	405s	484	408s	492	396m	493	400m	477	416m	517	412w		429m		
				358sh		369sh										434w	IR	Bending (ν_4) and
	444L		460L		471L		482L		485L		487L		502L(531L)		540L	376sh		torsional modes
312s	313T	308s	319T	298s	325T	315s	340T	306s	355T	322s	353T	332s	360T(389T)	280s	401T	357s		
												283s				322s		
																142sh	Raman	$T'(Ba^{2+}/Sr^{2+})$
106w	100	105m	102	103w	107	100m	108	103m	106	101m	109	115m	124	123w		135w		
	200L		183L		178L		216L		190L		248L	228m	117L			217m	IR	Translation of
175m	193T	175m	182T	174m	178T	216m	213T	174m	155T	213m	242T	185m	113T	—		182m		trivalent atoms
	124L		127L		129L		139L		114L		148L		166L(150L)		162L		IR	$T'(Ba^{2+}/Sr^{2+})$
115w	106T	114w	110T	114w	114T	117w	122T	115w	111T	121w	130T	127w	143T(138T)	126w	146T	144w		
																98vw		

similar to that observed in our spectra. However, the complementary Raman studies of $Pb(Sc_{1/2}Ta_{1/2})O_3$ showed that the rhombohedral distortion of the lattice should also lead to a splitting of the Raman bands [20]. Since we do not observe any splitting of the Raman bands, the contribution of the lattice distortion to the observed shoulders is weak, if any. Finally, it is worth noting that the former IR studies of perovskites indicated that there is a large frequency difference between the corresponding longitudinal and transversal bending and stretching modes [17, 21]. It is known that in such a case the shape of a powder IR spectrum strongly depends on the size and shape of the particles [12, 22]. We suppose, therefore, that this effect may significantly contribute to the observed IR shoulders, although some weak contributions due to impurities, lattice distortion and local symmetry breakdown cannot be excluded.

It is worth noting that there exists a clear correlation between the ionic radius of a lanthanide and yttrium cation and the wavenumbers of the A_{1g} stretching and F_{2g} bending modes observed for the compounds studied here. The wavenumbers decrease with increasing ionic radius of the cation, i.e. in the order Sm < Gd < Dy < Y (see table 3). This can be attributed to the decrease in the B–O bond length, where B denotes a site occupied statistically by rare earth or yttrium and Mo or W atoms, with increasing ionic radius. This behaviour is well predicted by the calculations except for the Sm-containing compound. It is worth noting that the same type of behaviour was previously observed for the $Sr(B'_{1/2}B''_{1/2})O_3$ compounds, where B′ = lanthanide ion and B″ = Nb, Ta [15]. Finally, we would like to mention that the calculations predict small LO–TO splitting (<20 cm^{-1}) for all the IR-active modes, except for the bending mode for which the LO–TO splitting can achieve even 150 cm^{-1} (see table 3). This result indicates a very significant contribution of long-range Coulomb interactions to this mode due to very large dipole moment changes during this vibration, as can be seen in figure 3.

3.3. $Ba(In_{2/3}W_{1/3})O_3$ and $Ba(In_{2/3}Mo_{1/3})O_3$ perovskites

As mentioned above, structural studies showed that BIMO crystallizes in a disordered $Pm\bar{3}m$ perovskite structure [4]. The polycrystalline BIWO obtained was found to be a mixture of both ordered ($Fm\bar{3}m$) and disordered ($Pm\bar{3}m$) structures [4]. The ordered structure of BIWO is isomorphic to the structure of ordered complex perovskites discussed above and, therefore, four IR and four Raman bands are expected to be observed for this phase (see the discussion in the previous paragraph). The disordered structure of the barium compound has only one $A(B'_{2/3}B''_{1/3})O_3$ formula in the unit cell. In this structure 1b sites are occupied by Ba^{2+} cations and 3d sites by oxygen atoms. The 1a sites are statistically occupied by In^{3+} and hexavalent atoms. Factor group analysis shows that the vibrations of oxygen atoms should give rise to $F_{2u} + 2F_{1u}$ modes, Ba^{2+} cations to a F_{1u} mode and In/W(Mo) atoms to a F_{1u} mode. Since a F_{2u} mode is both IR- and Raman-inactive and one of the F_{1u} modes corresponds to acoustic mode, one may expect to observe three modes active in the IR spectroscopy only. Recent studies and lattice dynamics calculations of disordered $LaAlO_3$, $LaMnO_3$ and $Pb(Sc_{1/2}Ta_{1/2})O_3$ showed that the highest wavenumber band (550–710 cm^{-1}) corresponds to the stretching vibration of the BO_6 octahedra, where B = Al, Mn, Sc/Ta, etc, the middle wavenumber mode (215–370 cm^{-1}) to the bending vibration of the BO_6 octahedra and the lowest wavenumber mode (60–220 cm^{-1}) to a vibration of the A ions (A = La, Pb, etc) against rigid BO_6 octahedron [17, 21, 23].

The IR spectrum of BIMO differs significantly from the spectra of the ordered perovskites discussed above. First, the stretching mode, corresponding to the ν_1 mode of a free octahedron, is observed at significantly higher energy, 643 cm^{-1}, than observed for the ordered rare earth perovskites (564–591 cm^{-1}). This shift indicates a significant shortening of the In/Mo–O

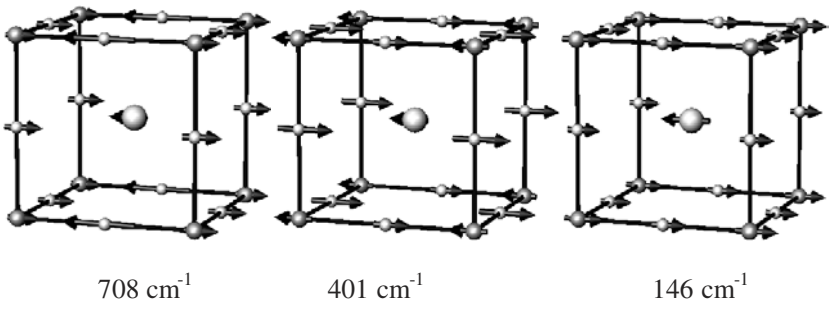

Figure 4. Calculated frequencies and displacement vectors for the representative perovskite crystallizing in the $Pm\bar{3}m$ structure ($Ba(In_{2/3}Mo_{1/3})O_3$). The Ba and B = In/Mo ions are situated at the centre and corners of the cube, respectively.

bond lengths in BIMO when compared to the Ln/Mo–O bond for the rare earth perovskites, in agreement with the structural studies which showed that this bond length shortens from 2.167 Å for BYMO to 2.083 Å for BIMO [4]. Only one band at 644 cm^{-1}, which could be assigned to the stretching mode (see table 3 and figure 4), is observed also for BIWO in spite of the fact that our previous HREM and XRD studies showed that this sample contains both ordered (70%) and disordered phases (21%) [4]. This feature can be attributed to the overlapping of the bands originating from the two phases and it shows that the observed shift of this band for both BIWO and BIWO towards higher energy does not depend on the ordering of the cations but can be attributed entirely to the effect of the much smaller ionic size of In(III), when compared to the ionic radii of the rare earth and yttrium ions. This behaviour is well predicted by the lattice dynamical calculations (see table 3). Second, the two bands observed at around 300 and 200 cm^{-1} for the ordered perovskites seem to merge into one very broad band for the disordered BIMO, observed at around 280 cm^{-1}. This band can be assigned, according to the calculations, to the bending mode (see figure 4). However, it seems that some weak band around 180 cm^{-1} is still present in the spectrum and an additional band appears around 380 cm^{-1}. The IR spectrum of BIWO shows very clearly the presence of the band around 185 cm^{-1} and the broad bending band shows the presence of some shoulders. The 185 cm^{-1}, can be assigned to the translation of tri- and hexavalent atoms. This mode should be observed for the ordered, and not observed for the disordered, phase. Indeed, IR studies of $Pb(Sc_{1/2}Ta_{1/2})O_3$ showed that the intensity of this type of mode, corresponding in the case of $Pb(Sc_{1/2}Ta_{1/2})O_3$ to antiphase Sc–Ta vibrations and observed at 314 cm^{-1}, can be used to estimate the degree of local order in this sample [17]. Our result, showing the presence of a weak band around 180 cm^{-1} for BIMO and much stronger for BIWO, agrees with the structural studies, which showed that the BIWO sample contains a large amount (70%) of ordered phase [4]. However, they suggest also the presence of a small amount of an ordered phase for the BIMO sample. The third lowest wavenumber band is observed at 126 cm^{-1} for BIMO and 127 cm^{-1} for BIWO. The shape, wavenumber and bandwidths of these bands are very similar to those observed for the lowest wavenumber bands in the ordered perovskites. The calculations show that these bands can be assigned to coupled translational motions of Ba^{2+}, In^{3+} and Mo^{6+}/W^{6+} ions (see figure 4). The calculated wavenumbers of the modes involving large motions of Ba^{2+} ions are very similar both for ordered and disordered structures of BIWO (see table 3). This result shows, similar to the behaviour of the stretching mode discussed above, that the wavenumber of this IR band does not depend significantly on the ordering of cations and explains why only one band is observed around 127 cm^{-1} for the

mixture of ordered and disordered BIWO. The calculations show also that very large LO–TO splitting should be observed for the bending mode only (see table 3). This result is similar to that predicted for the ordered perovskites (see table 3). Finally, as mentioned above the bending band of BIWO shows the presence of some shoulders and the BIMO spectrum shows the presence of an additional band around 380 cm^{-1}. The presence of the 380 cm^{-1} band cannot be attributed to the presence of an ordered phase since no similar band is observed for the BIWO sample, which contains a large amount of ordered phase. We suppose, therefore, that this band and the discussed shoulders have the same origin as the shoulders observed in the 358–369 cm^{-1} range for the ordered BDMO and BYMO samples and can be explained in the same way as discussed in the previous paragraph of the present paper.

The Raman spectrum of BIWO shows the presence of three bands, which could be assigned in the same way as those observed for the ordered rare earth and yttrium perovskites. These modes, except for the lowest wavenumber one, show a significant shift towards higher wavenumbers when compared to the respective modes of the rare earth and yttrium compounds. This behaviour can be attributed to the large difference between ionic radii of In^{3+} and rare earth and yttrium ions. The bandwidths of the observed Raman bands are similar to those observed for the rare earth and yttrium perovskites. We suppose, therefore, that the observed Raman scattering may come from the ordered phase. This result is consistent with our former structural studies showing that the sample contains much more ordered than disordered phase [4]. Surprisingly, the Raman spectrum could also be recorded for the BIMO sample although our former structural studies could not reveal the presence of the $Fm\bar{3}m$ phase in the sample [4] and, therefore, no Raman modes should be observed since there are no Raman-active modes for the $Pm\bar{3}m$ structure. The appearance of Raman bands for the studied BIMO sample may indicate that it contains an admixture of the $Fm\bar{3}m$ phase, which could not be detected during the x-ray and HREM studies due to the low concentration of this phase. However, the appearance of forbidden Raman bands may also be explained in a similar way to that proposed for relaxor perovskites [1, 5, 18, 20, 24]. Two approaches are used to explain the appearance of Raman bands in disordered perovskites. The first approach assumes that disorder breaks down the selection rules and, as a result, a contribution to light scattering should appear from both IR-active and -silent modes. The second approach implies the existence of ordered regions with a particular symmetry that allows the appearance of Raman scattering. Since our Raman spectra do not show the presence of any bands corresponding to IR-active modes, we may exclude the first explanation. It seems, therefore, that the observation of Raman bands and the 185 cm^{-1} IR band for BIMO can be explained as a result of ordering, which leads to the $Fm\bar{3}m$ structure. The similarity of the Raman spectrum of the BIMO sample to the spectra of the ordered rare earth perovskites and the BIWO sample supports this conclusion. For example, all spectra show similar contours and, similar to the case of the rare earth compounds, a significant shift of the A_{1g} mode is observed when the W atoms are replaced by Mo atoms (see table 3). Although the observed spectral features suggest that the Raman bands may come from the ordered $Fm\bar{3}m$ structure and may be attributed to either ordered regions embedded in the disordered matrix or the presence of ordered crystallites in the sample studied, two observations seem to support the former explanation. First, since no ordered crystallites could be detected by x-ray and HREM, the concentration of the $Fm\bar{3}m$ phase in the sample studied should be very small. The observation of a strong Raman signal is not consistent with the small content of this phase. Second, the comparison of the Raman spectra of BIMO and BIWO shows that the observed bands for the BIMO samples are much broader than those measured for the BIWO sample. The bandwidths of the 804–842, 416–412 and 115–123 cm^{-1} bands increase from 39, 27 and 6 cm^{-1} for BIWO to 55, 66 and 22 cm^{-1} for BIMO. This behaviour is not consistent with the assumption that the signal of BIMO comes from the ordered crystallites

since, in this case, one would expect to observe bands of similar bandwidths to those found for BIWO. The observed increase of the bandwidth for BIMO could be, however, explained assuming that the signal comes from the ordered regions embedded in the disordered matrix, since the studies of many perovskites showed that the bandwidth increases with the decrease of the degree of order and size of the ordered domains [5, 15, 24]. Moreover, the decrease of order was shown to result in a significant decrease of the intensity ratio of the ∼410 cm^{-1} (A_{1g}) and ∼800 cm^{-1} (F_{2g}) modes [15]. Our Raman spectra show very clearly this type of behaviour for the BIMO compound (see figure 1).

3.4. $Sr(In_{2/3}W_{1/3})O_3$ perovskite

The strontium compound, although it also crystallizes in a disordered structure, is characterized by lower *Pnma* symmetry. This structure belongs to the family of rotationally distorted perovskites with Galzer's notation ($a^-b^+a^-$) [25]. It can be obtained from the simple perovskite structure by two consequent rotations of BO_6 octahedra and it has been found for a number of perovskites such as $LaMnO_3$, $YAlO_3$, $YCrO_3$, etc [23, 26]. Since the unit cell contains four formula units, there are 60 Γ-point phonons corresponding to vibrations of Sr^{2+} cations ($2A_g + A_u + B_{1g} + 2B_{1u} + 2B_{2g} + B_{2u} + B_{3g} + 2B_{3u}$), oxygen atoms ($5A_g + 4A_u + 4B_{1g} + 5B_{1u} + 5B_{2g} + 4B_{2u} + 4B_{3g} + 5B_{3u}$) and translational motions of In/W atoms ($3A_u + 3B_{1u} + 3B_{2u} + 3B_{3u}$). Because of a large number of modes the detailed assignment could be achieved only with the help of lattice dynamical calculations. In order to perform such calculations it would be, however, necessary to know the symmetries of the vibrational modes derived from polarized IR and Raman spectra of a single crystal. Unfortunately, single crystals of SIWO are not available and, therefore, it was not possible to use lattice dynamical calculations to obtain the reliable assignment of vibrational modes. We had, therefore, to base our assignments on comparison with the spectra of the cubic perovskites discussed above. The inspection of the measured spectra shows that they are very similar to the spectra of cubic perovskites except for the fact that a clear splitting of some bands is observed. This result shows that the vibrational modes can still be correlated with the modes of a free octahedron. We may assign, therefore, the 844 cm^{-1} mode to the totally symmetric stretching mode (ν_1 of a free octahedron). This and many other modes which are not active in the disordered cubic phase arise from the (1/2, 1/2, 1/2), (1/2, 0, 1/2) and (0, 1/2, 0) points of the cubic Brillouin zone. As far as the modes corresponding to the $\nu_2(E_g)$ stretching mode of a free octahedron are concerned, it is not clear whether the weak band at 538 cm^{-1} can be assigned to this vibration or to some impurity. The measured spectra show that the mode corresponding to the $\nu_3(F_{1u})$ mode of a free octahedron, observed around 640 cm^{-1}, shows a very clear triplet structure. This splitting, arising from lifting of the degeneracy for this mode due to symmetry lowering, is relatively large (78 cm^{-1}). Since it is obvious that the splitting is a measure of the deviation of the structure from the ideal cubic one, the observation of a large splitting indicates a large distortion of the structure, in agreement with the structural studies presented in [4]. Similar splitting is observed also for other modes degenerated in the cubic phase, i.e. for the bending modes observed in the 440–320 cm^{-1} range (ν_4 and ν_5 of a free octahedron) and the translational mode of In/W atoms, observed at 182 and 217 cm^{-1}. The energy of these modes is similar to that found for the ordered perovskites discussed in the previous section of this paper. It should be noticed, however, that the studies of other orthorhombically distorted perovskites revealed the presence in the 450–300 cm^{-1} region of new IR bands, not observed for the cubic phase, which were assigned to torsional modes [21]. We assign, therefore, the IR bands in the 440–320 cm^{-1} range to both bending and torsional modes. The performed studies also show that lowest-wavenumber Raman and IR modes are

observed for SIWO at significantly higher wavenumbers, 135–142 (Raman) and 144 cm^{-1} (IR), than for the barium-containing compounds (100–123 and 114–127 cm^{-1}, respectively). This shift clearly indicates that these modes are connected with the translational motions of divalent cations.

4. Conclusions

In summary, we studied the Raman and IR phonons of ordered ($Fm\bar{3}m$) and disordered ($Pm\bar{3}m$ or $Pnma$) perovskites and made an assignment of the experimentally observed bands to specific motions of atoms. The presented studies show that the vibrational properties of these compounds, except for BIMO, can be well correlated with their average crystal structure. The differences in the crystal structure are reflected through different selection rules. In particular, a very clear splitting of degenerate modes due to orthorhombic distortion is observed for the SIWO perovskite. The present studies revealed also the presence of modes for the BIMO structure, forbidden by selection rules, described by an average disordered structural model (group $Pm\bar{3}m$) with a random distribution of In^{3+} and Mo^{6+} ions on the B sites. Our present study with the use of IR and Raman techniques, which are known to be sensitive to the local atomic environment, suggest that the appearance of these modes may be explained by the presence of 1:1 ordered domains embedded in the disordered $Pm\bar{3}m$ matrix. These studies suggest that BIMO and BIWO can be obtained in both ordered and disordered forms, depending on the thermal treatment. They seem, therefore, to behave in a similar way as the well known $Pb(In_{1/2}Nb_{1/2})O_3$, $Pb(Sc_{1/2}Nb_{1/2})O_3$ and $Pb(Sc_{1/2}Ta_{1/2})O_3$ relaxors. This can be related to the fact that the chemical difference between Nb^{5+} and W^{6+} ions is small and therefore similar behaviour can be expected for In–Nb and In–W compositions.

Acknowledgments

This study was financially supported by CONACYT (project 31198U) and the Polish Committee for Scientific Research, grant no 7 TO8D 042 19. The authors thank Dr T Misiaszek for recording the Raman spectra of indium-containing compounds.

References

[1] Ye Z-G 1998 *Key Eng. Mater.* **155/156** 81
[2] Rao C N R and Raveau B (ed) 1998 *Colossal Magnetoresistance, Charge Ordering and Related Properties of Manganese Oxides* (Singapore: World Scientific)
[3] Anderson M T, Greenwood K B, Taylor G A and Poeppelmeier K R 1993 *Prog. Solid State Chem.* **22** 197
[4] Fuentes A F, Hernández-Ibarra O, Mendoza-Suarez G, Escalante-García J I, Boulahya K and Amador U 2003 *J. Solid State Chem.* **173** 319
[5] Siny I G, Katiyar R S and Bhalla A S 1998 *J. Raman Spectrosc.* **29** 385 and references therein
[6] Ye Z-G, Toda K and Sato M 1998 *J. Korean Phys. Soc.* **32** S1028
[7] Feng L and Ye Z-G 2002 *J. Solid State Chem.* **163** 484
[8] Pechini M 1967 Method of preparing lead and alkaline-earth titanates and niobates and coating method using the same to form a capacitor *US Patent Specification* 3330697
[9] Fuentes A F, Garza-Garcia M, Escalante-García J I, Mendoza-Suárez G, Boulahya K and Amador U 2003 *J. Solid State Chem.* **175** 298
[10] Nozaki R, Kondo J N, Hirose C, Domen K, Wada A and Morioka Y 2001 *J. Phys. Chem.* B **105** 7950 and references therein
[11] Tanaka H, Tabata H, Ota K and Kawai T 1996 *Phys. Rev.* B **53** 14112
[12] Ligeois-Duyckaerts M and Tarte P 1973 *Spectrochim. Acta* A **30** 1771
[13] Tao R, Guo A R, Tu C-S, Siny I and Katiyar R S 1996 *Ferroelectr. Lett.* **21** 79

[14] Gregora I, Petzelt J, Pokorny J, Vorlicek V and Zikmund Z 1995 *Solid State Commun.* **94** 899
[15] Ratheesh R, Berge B, Wahlbrink Th, Haeuseler H, Rühl E, Blachnik R, Balan P, Santha N and Sebastian M T 2000 *J. Appl. Phys.* **88** 2813
[16] Daturi M, Busca G, Borel M M, Leclaire A and Piaggio P 1997 *J. Phys. Chem.* **101** 4358
[17] Petzelt J, Bixaderas E and Pronin A V 1998 *Mater. Sci. Eng.* B **55** 86
[18] Siny I G and Katiyar R S 1998 *Ferroelectrics* **206** 307
[19] Reanay J M, Petzelt J, Voitsekhovskii V V, Chu F and Setter N 1994 *J. Appl. Phys.* **76** 2086
[20] Bismayer U, Devarajan V and Groves P 1989 *J. Phys.: Condens. Matter* **1** 6977
[21] Abrashev M V, Litvinchuk A P, Iliev M N, Meng R L, Popov V N, Ivanov V G, Chakalov R A and Tomsen C 1999 *Phys. Rev.* B **59** 4146
[22] Ruppin R and Engelman R 1970 *Rep. Prog. Phys.* **33** 149
[23] Granado E, Moreno N O, Garcia A, Sanjurjo J A, Rettori C, Torriami I, Oseroff S B, Neumeier J J, McClellan K J, Cheong S-W and Yokura Y 1998 *Phys. Rev.* B **58** 11435
[24] Jiang F and Kojima S 2000 *J. Appl. Phys.* **88** 3608
[25] Glazer A M 1972 *Acta Crystallogr.* B **28** 3384
[26] Iliev M N, Abrashev M V, Lee H-G, Popov V N, Sun Y Y, Thomsen C, Meng R L and Chu C W 1998 *Phys. Rev.* B **57** 2872